

N O T I C E

THIS DOCUMENT HAS BEEN REPRODUCED FROM
MICROFICHE. ALTHOUGH IT IS RECOGNIZED THAT
CERTAIN PORTIONS ARE ILLEGIBLE, IT IS BEING RELEASED
IN THE INTEREST OF MAKING AVAILABLE AS MUCH
INFORMATION AS POSSIBLE

NASA TECHNICAL MEMORANDUM

NASA TM-82428

FRACTURE ANALYSIS OF HPOTP BEARING BALLS

By Biliyar N. Bhat
Materials and Processes Laboratory

May 1981

NASA



*George C. Marshall Space Flight Center
Marshall Space Flight Center, Alabama*

(NASA-TM-82428) FRACTURE ANALYSIS OF HPOTP
BEARING BALLS (NASA) 27 F HC A03/ME A01
CSCL 131

N81-28442

Unclass

G3/37 26909

**NASA TECHNICAL
MEMORANDUM**

NASA TM-82428

**FRACTURE ANALYSIS OF HPOTP
BEARING BALLS**

**By Biliyar N. Bhat
Materials and Processes Laboratory**

May 1981

NASA

*George C. Marshall Space Flight Center
Marshall Space Flight Center, Alabama*

1. REPORT NO. NASA TM-82428	2. GOVERNMENT ACCESSION NO.	3. RECIPIENT'S CATALOG NO.	
4. TITLE AND SUBTITLE Fracture Analysis of HPOTP Bearing Balls		5. REPORT DATE May 1981	6. PERFORMING ORGANIZATION CODE
7. AUTHOR(S) Bilivar N. Bhat		8. PERFORMING ORGANIZATION REPORT #	
9. PERFORMING ORGANIZATION NAME AND ADDRESS George C. Marshall Space Flight Center Marshall Space Flight Center, AL 35812		10. WORK UNIT NO.	11. CONTRACT OR GRANT NO.
12. SPONSORING AGENCY NAME AND ADDRESS National Aeronautics and Space Administration Washington, D.C. 20546		13. TYPE OF REPORT & PERIOD COVERED Technical Memorandum	
15. SUPPLEMENTARY NOTES		14. SPONSORING AGENCY CODE	
15. SUPPLEMENTARY NOTES Prepared by Materials and Processes Laboratory, Science and Engineering.			
16. ABSTRACT <p>This report presents the fracture analysis conducted on four HPOTP (High Pressure Oxygen Turbopump) bearing balls from the SSME (Space Shuttle Main Engine). Non-destructive evaluation, optical microscopy, and transmission microscopy techniques were used in the analysis. The results showed that the cracks are initiated at or close to the ball surface under conditions of high cyclic stresses and high coefficient of friction. The cracks lead to spalls and subsequent crack propagation seems to occur by fatigue mode under concentrated loading of cyclic nature.</p>			
17. KEY WORDS		18. DISTRIBUTION STATEMENT Unclassified - Limited	
19. SECURITY CLASSIF. (of this report) Unclassified	20. SECURITY CLASSIF. (of this page) Unclassified	21. NO. OF PAGES 26	22. PRICE NTIS

ACKNOWLEDGMENTS

The author wishes to acknowledge the valuable help received from the following personnel of the Materials and Processes Laboratory, Marshall Space Flight Center: W.R. DeWeese, in metallography; G.R. Marsh, in electron microscopy; and J.R. Sandlin, in preparing illustrations. I would also like to thank F. Dolan for his technical assistance and encouragement, and J. Knadler and B. Bankston for their help in nondestructive examination.

TABLE OF CONTENTS

	Page
INTRODUCTION.....	1
EXAMINATION PROCEDURE AND RESULTS.....	1
DISCUSSION	2
CONCLUSIONS	4
REFERENCES	5

LIST OF ILLUSTRATIONS

Figure	Title	Page
1.	Photomicrograph of Ball No. 1 From HPOTP 2502, Engine 0008	6
2.	Subsurface crack in HPOTP 2502 bearing ball from Engine 0008	7
3.	Surface cracks in HPOTP 2502 bearing ball from Engine 0008	8
4.	Surface crack in HPOTP 2502 bearing ball from Engine 0008	9
5.	(A) Photograph of Ball No. 2 from HPOTP 9008, Engine 2004. (B) Photomicrograph of section of ball through the crack	10
6.	(A) Photomicrograph of Ball No. 3 from HPOTP 9008, Engine 2502. (B) Cross section of the ball at top.....	11
7.	Crack in spalled ball from HPOTP 9008 bearing in Engine 2502	12
8.	Shallow surface crack in spalled ball from HPOTP 9008 bearing in Engine 2502	13
9.	Cracks in spalled ball from HPOTP 9008 bearing in Engine 2502	14
10.	Cross section of spalled ball from HPOTP 9008 bearing in Engine 2502	15
11.	Deep cracks in spalled ball from HPOTP 9008 bearing in Engine 2502	16
12.	Cross section of spalled Ball No. 4 from HPOTP 9008 bearing from Engine 2004	17
13.	Deep crack in HPOTP 9008 bearing ball from Engine 2004	18
14.	Deep crack in HPOTP 9008 bearing ball from Engine 2004	19
15.	Shallow crack in HPOTP 9008 bearing ball from Engine 2004	20
16.	TEM photomicrographs of fractured surface in HPOTP 9008 bearing ball from Engine 2004	21

TECHNICAL MEMORANDUM

FRACTURE ANALYSIS OF HPOTP BEARING BALLS

INTRODUCTION

The High Pressure Oxygen Turbopump (HPOTP) bearings of the Space Shuttle Main Engine (SSME) have been known to crack and spall prematurely [1,2]. In order to increase the life and reliability of the SSME, it is important to understand and correct this problem. Many attempts have been made to determine the cause of bearing failures. For example, a detailed examination of failed balls, races and cages, and a stress analysis were conducted by Battelle Columbus Laboratories [3]. Furthermore, analyses of wear in HPOTP bearings were made by NASA personnel at MSFC. These analyses seem to indicate that the bearings are subjected to variable, sometimes very high [estimated at approximately 4545-kg (10,000-lb)] transient axial loads, which are believed to cause the bearings to crack by fatigue. Based on the depth of the fatigue cracks, the maximum Hertzian stress in the bearings was estimated to be greater than the design 186 GPa (270,000 psi) [3]. While steps are being taken to reduce the high transient axial loads, efforts are continuing to improve our understanding of the bearing failure. As a part of these efforts, a fracture analysis of selected balls from HPOTP bearings was conducted at Materials and Processes Laboratory. Both surface and subsurface cracks were characterized and attempts were made to determine the possible causes of crack initiation and propagation. The details of these analyses are presented in the following sections.

EXAMINATION PROCEDURE AND RESULTS

A total of four HPOTP No. 3 bearing balls were examined, two with spalls and two without. The origin and surface characteristics of these balls are given in Table 1. Ball No. 1 showed no visible surface cracks or spalls but had visible wear tracks and numerous shallow pits (Fig. 1). In order to determine if the ball had any subsurface cracks, a nondestructive evaluation technique was used. In this technique, the ball was placed in an eddy current probe operating at 500 KHz and tested. A subsurface flaw was detected. The flaw was located on the wear tracks. Subsequent to the eddy probe examination, the ball was mounted in epoxy and sectioned parallel to the wear track, using a diamond cut-off device. The cross section was polished, etched in Vilella's reagent [4] and examined under an

optical microscope for cracks. Any cracks observed were photographed. Then a 0.25 mm (0.010 in.) thickness was removed by grinding and the sample was again polished, etched and examined for cracks. This procedure was continued until the wear tracks were ground off completely.

Photomicrographs of cracks in ball No. 1 are presented in Figures 2 through 4. Figure 2 shows two photomicrographs of a subsurface crack at two different positions. The position 2 is 0.25 mm (0.010 in.) from position 1. This crack was correctly located by the eddy probe. Figures 3 and 4 show different types of surface cracks present in the ball. It should be noted that all these cracks are very shallow, less than .025 mm (0.001 in.) deep. They appear to meet the surface at relatively small angles (approximately 20°).

Figure 5 shows a surface crack in ball No. 2 (Table 1). Figure 6(A) is a photomicrograph of ball No. 3 (Table 1), and Figure 6(B) is a cross section of that ball. The photomicrographs of cracks in ball No. 3 are given in Figures 7, 8, and 9. Figure 10 is the second half of ball No. 3 in Figure 6. Figure 11 is a photomicrograph of the crack from area A in Figure 10. It should be noted that cracks in the photomicrographs appear to be mirror images of cracks in the corresponding photomicrographs because different metallographs were used in the two cases.

Figure 12 is a cross section of ball No. 4 from HPOTP 9008, No. 3 bearing from engine 2004. A deep crack, nearly 2.3 mm (0.090 in.) deep, is visible at area A. Figure 13 is a high magnification photomicrograph of a crack at area A in Figure 12. Figure 14 is a photomicrograph of a crack at area B in Figure 12. Figure 15 is a photomicrograph of a shallow crack in area C, (Fig. 12) away from the heavily spalled areas A and B. This crack appears to have originated at a shallow spall and then propagated inwards at a continuously increasing angle. Extensive branching has occurred with cracks meeting at approximately 90°. The cracks appear to be oriented at 45° to the surface. Significance of these angles is discussed in the next section.

The crack A in Figure 12 was opened and the fractured surface was carbon replicated for examination in the transmission electron microscope. Two TEM photomicrographs of the fractured surface are shown in Figure 16. Parallel lines, resembling fatigue striations, are observed. Such striations were observed in different parts of the fractured surface.

DISCUSSION

It is significant that the subsurface crack in ball No. 1 (Fig. 2) was correctly located by the eddy probe technique. This result shows that it is possible to determine the subsurface cracks in balls without having to section them. Hence eddy current probe technique may be used to nondestructively identify balls having subsurface flaws existing at the time of manufacture or subsequently induced in operation.

It is also significant that the subsurface crack was actually located under the wear track. This location is to be expected because the bearing material under the wear track is subjected to cyclic stresses. According to the Palmgren theory [5] fatigue cracks initiate under stress at locations of maximum shear stress which is usually subsurface, typically 0.075 to 0.203 mm (0.003 to 0.008 in.), depending on the magnitude of Hertzian stress [3]. Under conditions of pure rolling, high stresses initiate fatigue cracks at deep locations. With the addition of frictional or sliding forces, planes of maximum shear stress move closer to the surface [6]. Sliding forces of sufficient magnitude can cause cracks to originate at the surface and significantly reduce bearing life. The cracks in Figure 3 appear to be surface initiated. The cracks shown in Figure 4 are in advanced stages and it is difficult to tell their origin. Interestingly, all cracks in this ball were very shallow, less than 0.001 in. from the surface. This result suggests two possible mechanisms of cracking: (1) Hertzian stresses are very low such that crack initiation occurs at very shallow depths; (2) Hertzian stresses are high but the coefficient of friction is also high such that the plane of maximum shear stress is very close to the surface. The author favors the latter mechanism because, if the Hertzian stresses were indeed low, the bearing life would have been very long (hundreds of hours). However, the ball in question had seen only 1904 sec of operation in the turbopump (7) and subsurface crack initiation is not expected in such a short time period under normal loading conditions. On the other hand, surface cracks are expected to occur in a short time under abnormally high loading conditions in combination with poor lubrication (high coefficient of friction). Therefore, it appears that the cracks in this ball were initiated under conditions of high stresses and high coefficient of friction. The high coefficient of friction was probably due to the failure of teflon transfer film lubrication. If this hypothesis is correct, it should be possible to increase the life of this bearing by improving lubrication.

The crack in ball No. 2 (Fig. 5) appears to propagate nearly perpendicular to the surface. The reason for this kind of crack is not well understood. It is possible that this was a preexisting crack.

The crack in ball No. 3 (Fig. 7) appears to run parallel to the ball surface and is approximately 0.18 mm (0.007 in.) deep. The fracture at the spalled edge is nearly perpendicular to the surface. This crack configuration is consistent with a subsurface crack initiated under high Hertzian stresses, >3.8 GPa (550 ksi) [3]. The crack in Figure 8, on the other hand, appears to have initiated at a shallow spall (at the upper right hand corner of the Figure), and propagated inward at an increasing angle. Figure 9 shows a more advanced stage of spalling in which some material from the surface has been removed and cracks have propagated deeper inside. The deep crack has two branches at right angles and both appear to be at approximately 45° to the surface. This type of crack pattern could be a result of concentrated loading [8]. Another example of a 45° crack pattern is shown in Figure 15. Here again, the crack appears to have originated at a shallow spall and propagated inwards at an increasing angle. The branches are at 90° to each other and at 45° to the surface.

Examples of very deep cracks are given in Figure 11, 13, and 14 (balls No. 3 and No. 4). All these cracks appear to have originated in heavily spalled areas. The crack propagation patterns seem to follow the shear trajectories predicted by a stress model based on concentrated loading [8]. Further analytical work is needed to accurately predict the crack propagation patterns. TEM photomicrographs of a carbon replica of the fractured surface of the crack in Figure 13 are shown in Figure 16. This figure shows striations that are typical of crack growth by fatigue mode. The striation spacing is approximately 0.03μ . This spacing corresponds to approximately 75,000 cycles for the crack to grow to a length of 2.3 mm (0.090 in.). This result translates into approximately 15,000 revolutions or 30 sec of running time for the HPOTP at 30,000 rpm. The actual running time is difficult to predict and might be longer than the estimated 30 seconds, but the result suggests that crack propagation could occur in a relatively short time.

Considering the crack trajectories, deep spalls, and shallow spalls, the following scenario of HPOTP bearing ball failure results. Subsurface and surface cracks are initiated under high Hertzian stresses combined with high coefficient of friction. The cracks lead to spalls. Deep cracks are initiated at the spalls under concentrated loading on the edge of the spalls. These cracks propagate rapidly by fatigue mode.

CONCLUSIONS

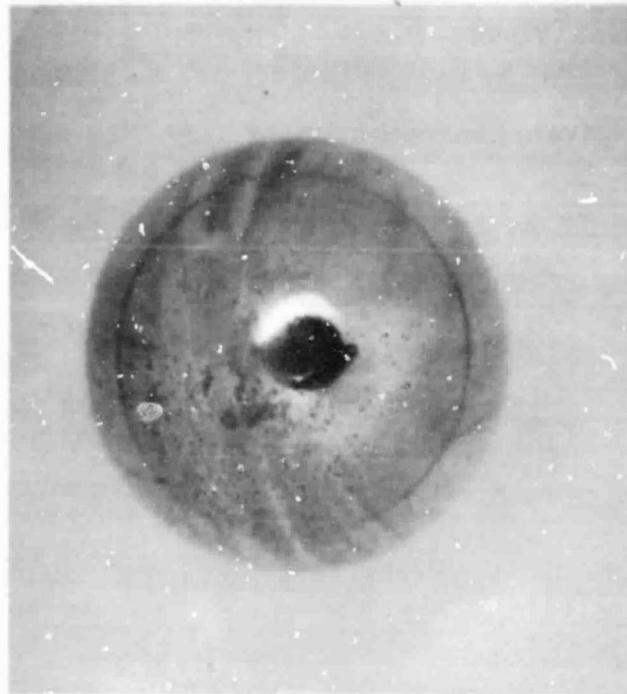
1. Crack initiation seems to occur at both surface and subsurface locations.
2. Cracks in unspalled balls are generally shallow, <0.025 mm (0.001 in.), but spalled balls have deep cracks, up to 2.3 mm (0.090 in.)
3. Crack growth seems to occur along shear trajectories corresponding to concentrated loading on the edge of spalls.
4. Crack initiation is apparently due to high Hertzian stresses combined with high coefficient of friction between balls and races. The high coefficient of friction is probably a result of poor lubrication.
5. Eddy current probe may be used to detect and locate subsurface cracks.

REFERENCES

1. F. Dolan: SSME Travel to Rocketdyne Division, Rockwell International, Canoga Park, CA. Memorandum to Dr. Gause, May 15, 1980.
2. F. Dolan: SSME Travel to Rocketdyne Division, Rockwell International, Canoga Park, CA. Memorandum to R. J. Schwinghamer, August 26, 1980.
3. K.F. Dufrane and J.W. Kannel: Evaluation of Space Shuttle Main Engine Bearings from High Pressure Oxygen Turbopump 9008, July 11, 1980. Final Report from Battelle to NASA/MSFC.
4. Atlas of Microstructures, Metals Handbook, Vol. 7, 8th Edition, American Society for Metals, 1972, p. 342.
5. G. Lundberg and A. Palmgren: Dynamic Capacity of Roller Bearings. Acta Polytech, No. 210, 1952.
6. Failure Analysis and Prevention, Metals Handbook, Vol. 10, 8th Edition, American Society for Metals, 1975, p. 152.
7. M. F. Butner: Turbine Bearings, HPOTP 2502, Engine 0008. Internal Letter to M. Pollack, Rockwell International, September 30, 1980.
8. A. Nunes, Private Communication.

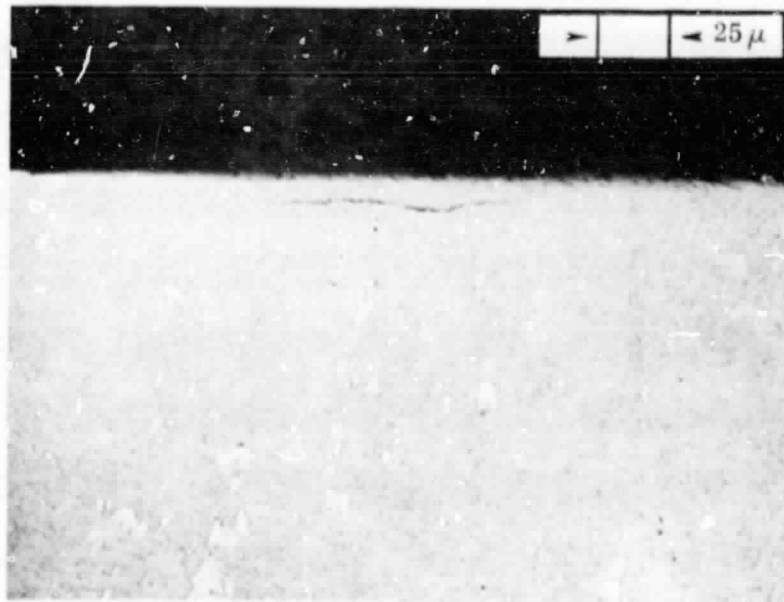
TABLE 1. SOME DETAILS OF THE HPOTP BEARING BALLS EXAMINED IN THIS REPORT

Ball No.	HPOTP	Engine	Surface Characteristics
1.	2502	0008	Two visible wear tracks; two pitted areas present on tracks (see Figure 1); no visible surface crack or spall.
2.	9008	2004	One surface crack; no visible spalls (see Figure 5).
3.	9008	2502	Heavy spalling (see Figure 6).
4.	9008	2004	Heavy spalling.



Mag. 4.5X

FIGURE 1. Photomicrograph of Ball No. 1 from HPOTP 2502, Engine 0008. Note the pits and wear tracks. The black dot was used to minimize glare. Photomicrographs of sections of this ball are given in Figures 2, 3, and 4.



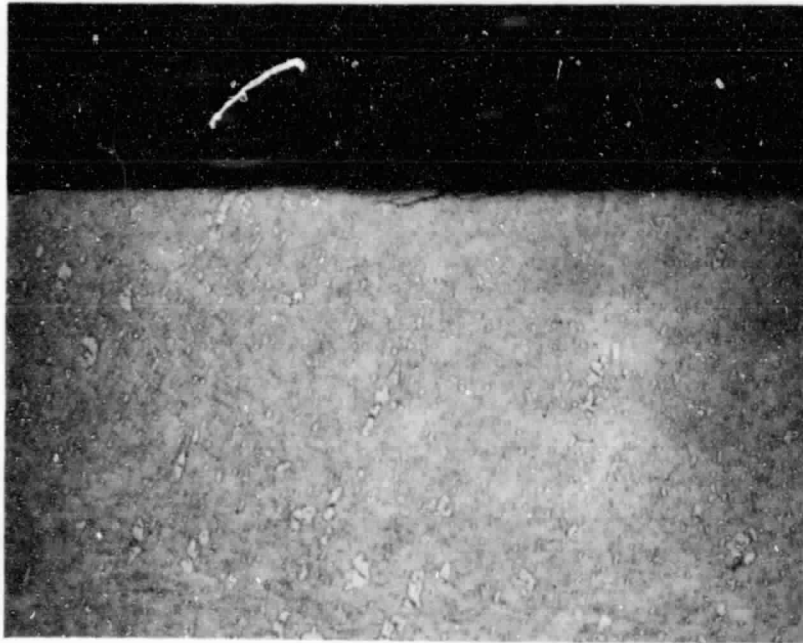
Position 1



Position 2

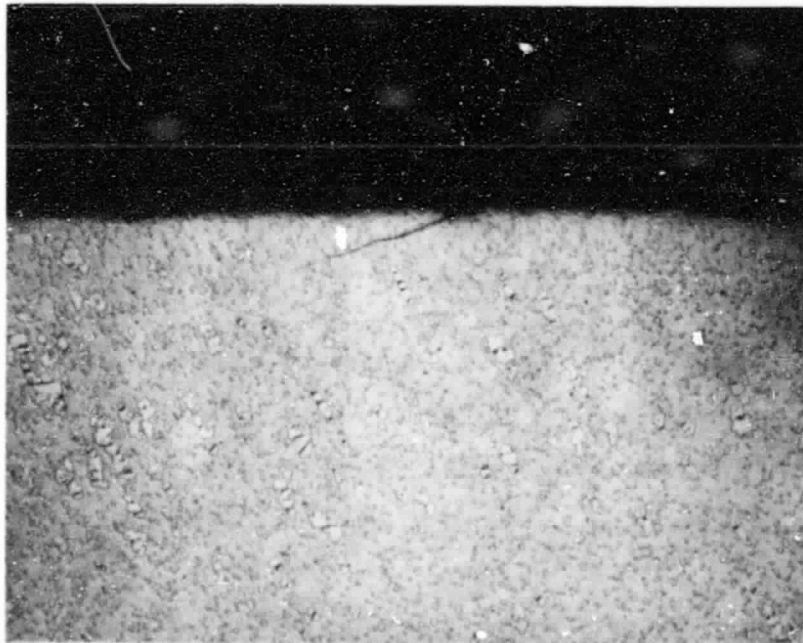
(.010 in. from Position 1)

Figure 2. Subsurface crack in HPOTP 2502 bearing ball from Engine 0008. Crack depth approximately 0.075 to 0.203 mm (0.0003 to 0.0008 in.)



A.

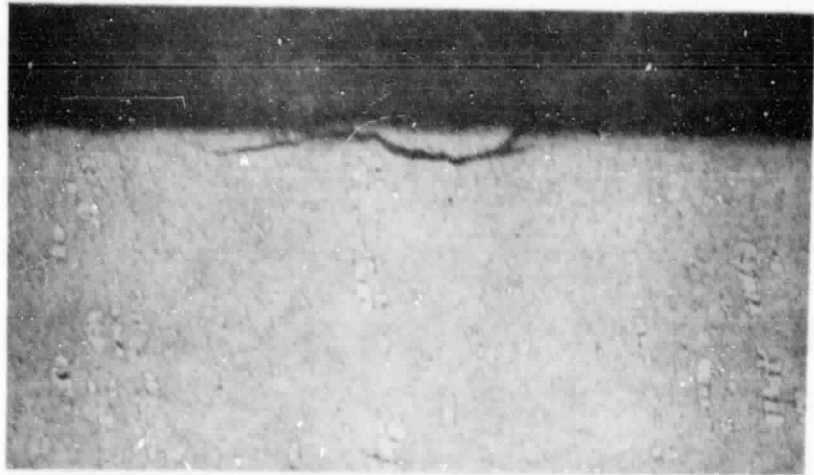
Mag. 400X



B.

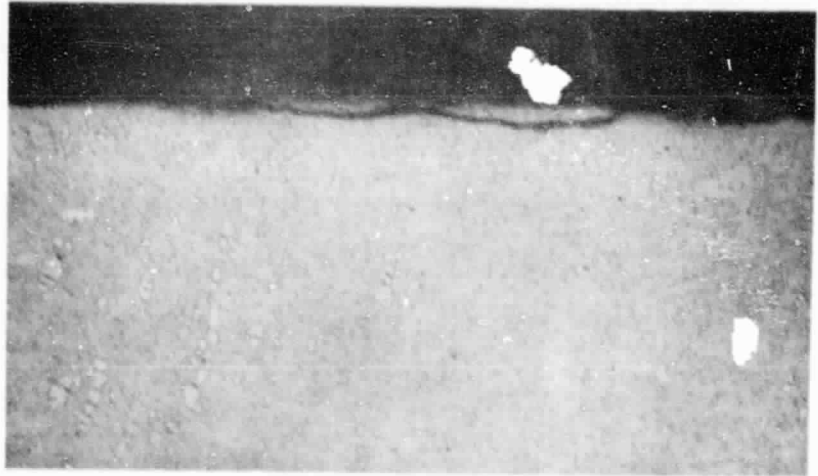
Mag. 400X

Figure 3. Surface cracks in HPOTP 2502 bearing ball from Engine 0008.



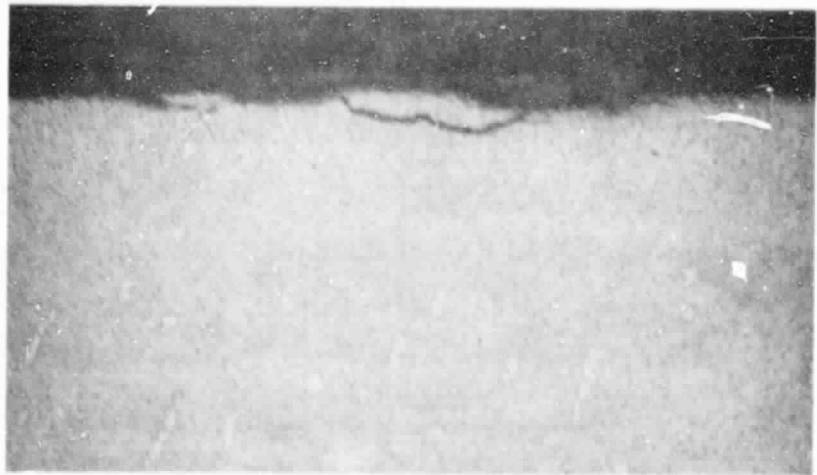
A.

Mag. 400X



B.

Mag. 400X

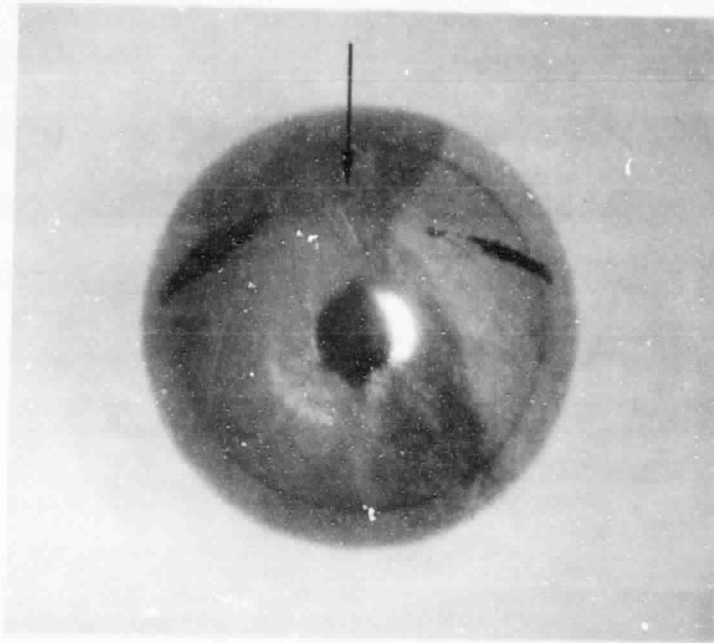


C.

Mag. 400X

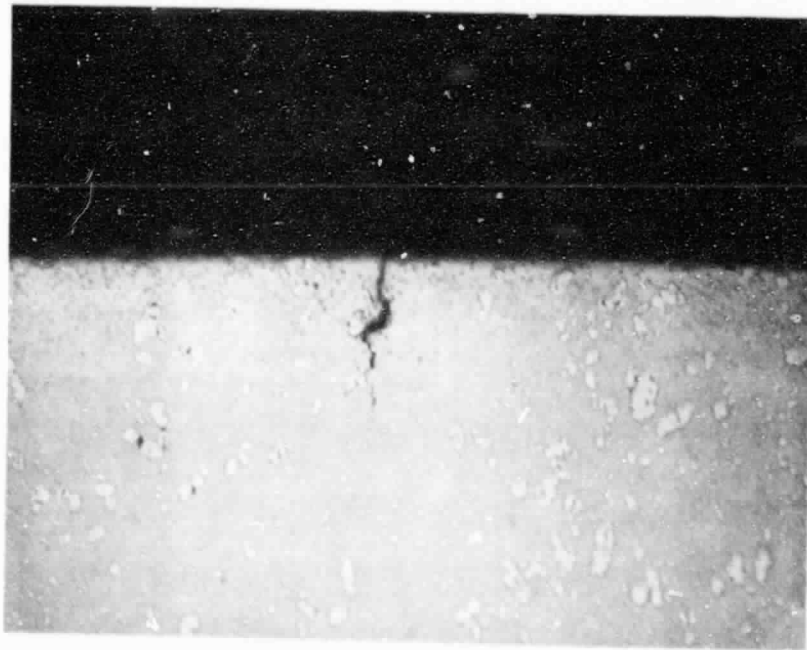
ORIGINAL PAGE IS
OF POOR QUALITY

Figure 4. Surface cracks in HPOTP 2502 bearing ball from Engine 0008.



A.

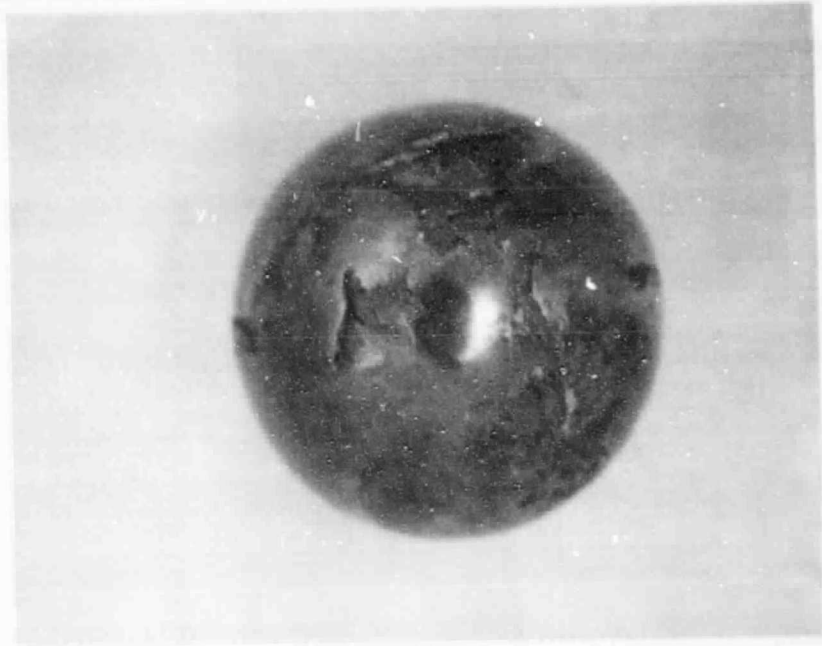
Mag. 4.5X



B.

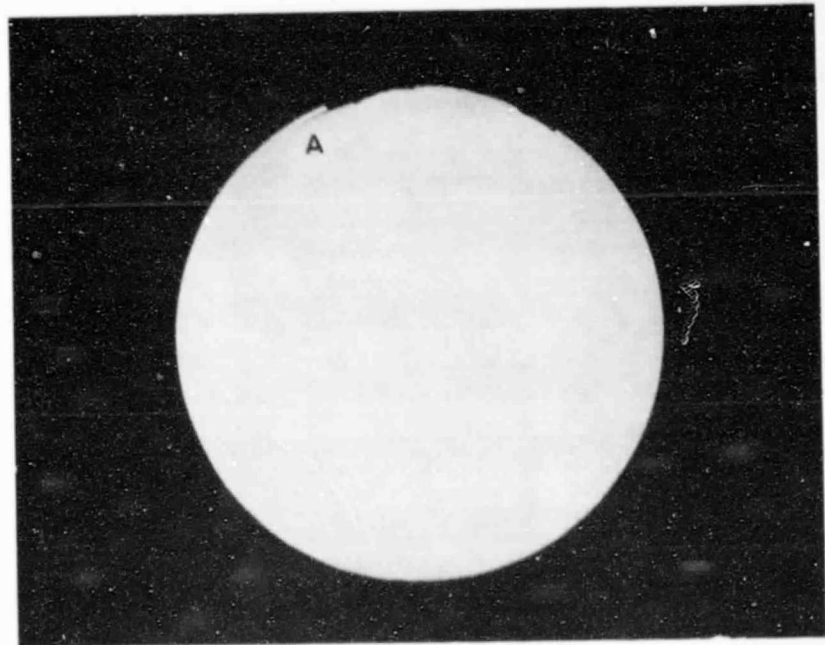
Mag. 400X

Figure 5. (A) Photograph of ball No. 2 from HPOTP 9008, Engine 2004. Note the surface crack. (B) Photomicrograph of section of ball through the crack. Crack depth approximately 0.05 mm (0.002 in.).



A.

Mag. 4.5X



B.

Mag. 5X

Figure 6. (A) Photomicrograph of ball No. 3 from HPOTP 9008, Engine 2502. (B) Cross section of the ball at top. Photomicrographs of this ball are shown in Figures 7 through 11.

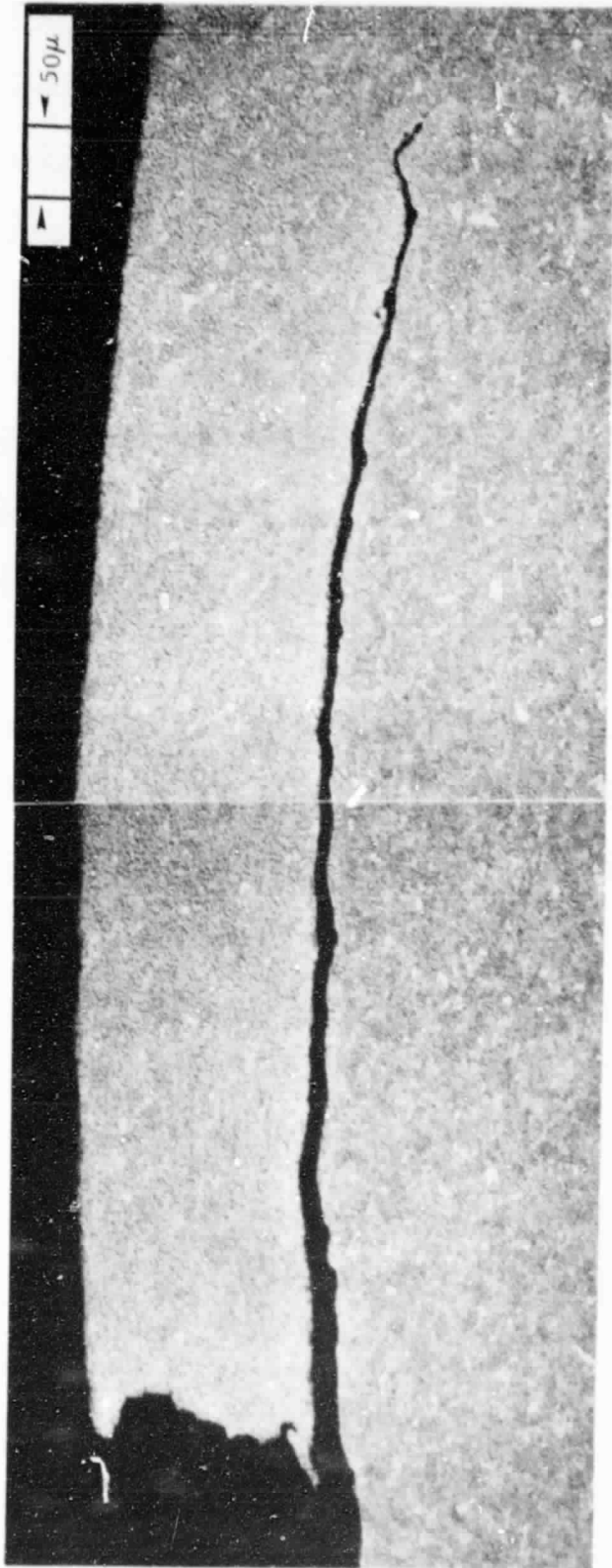


Figure 7. Crack in spalled ball from HPOTP 9008 bearing in Engine 2502 (area A in Figure 6).

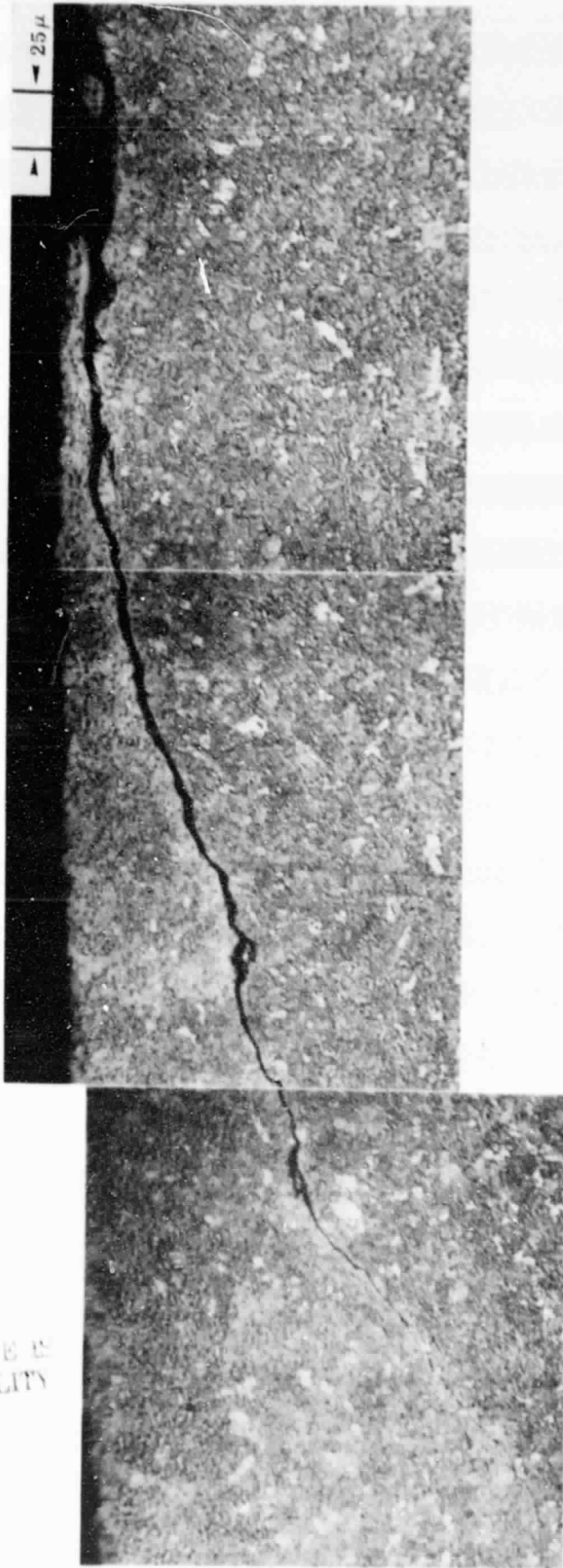


Figure 8. Shallow surface crack in spalled ball from HPOTP 9008 bearing in Engine 2502. Crack depth approximately 0.18 mm (0.007 in.).

ORIGINAL PAGE IS
OF POOR QUALITY

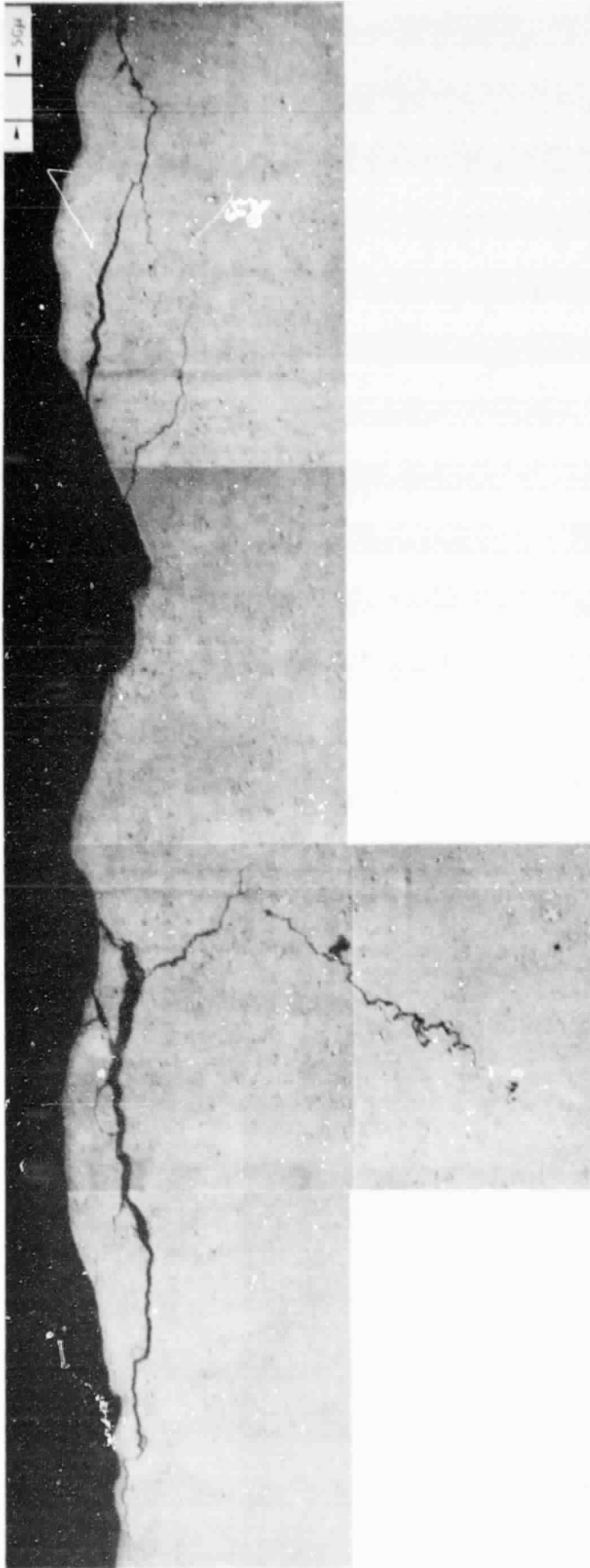


Figure 9. Cracks in spalled ball from HPOTP 9008 bearing in Engine 2502.

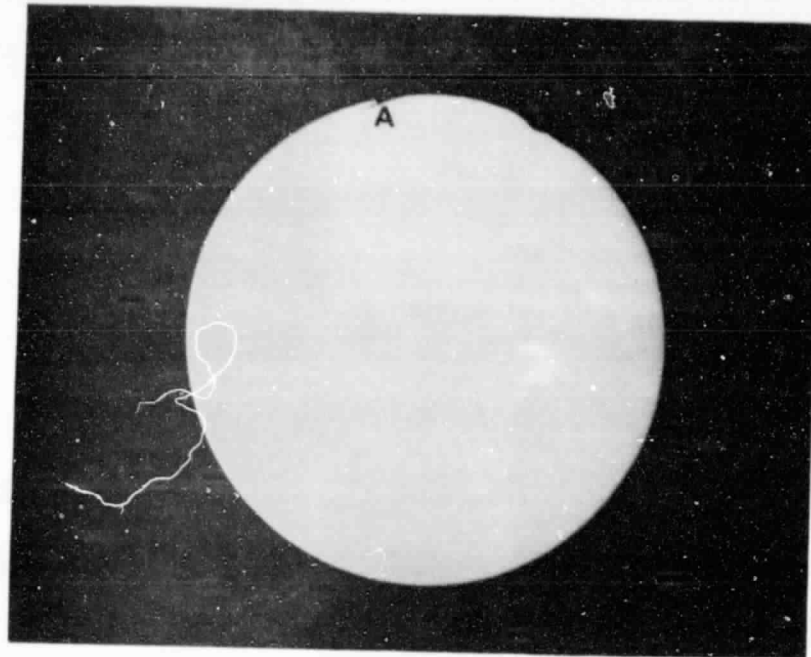


Figure 10. Cross section of spalled ball from HPOTP 9008 bearing in engine 2502. Crack in area A is shown in Figure 11. Original magnitude 5X.

ORIGINAL PAGE IS
OF POOR QUALITY

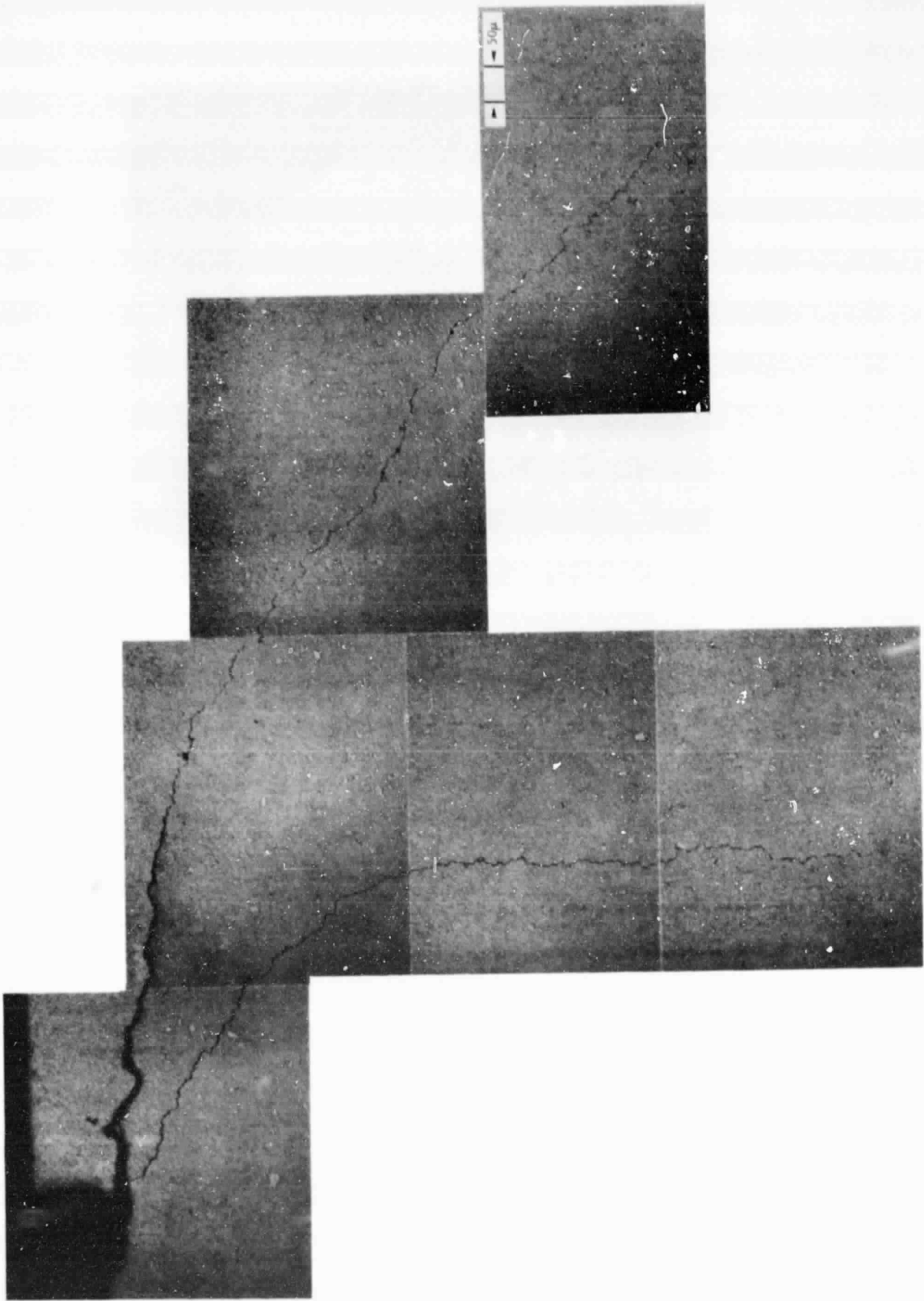


Figure 11. Deep cracks in spalled ball from HPOTP 9008 bearing in Engine 2502 (area A in Figure 10).

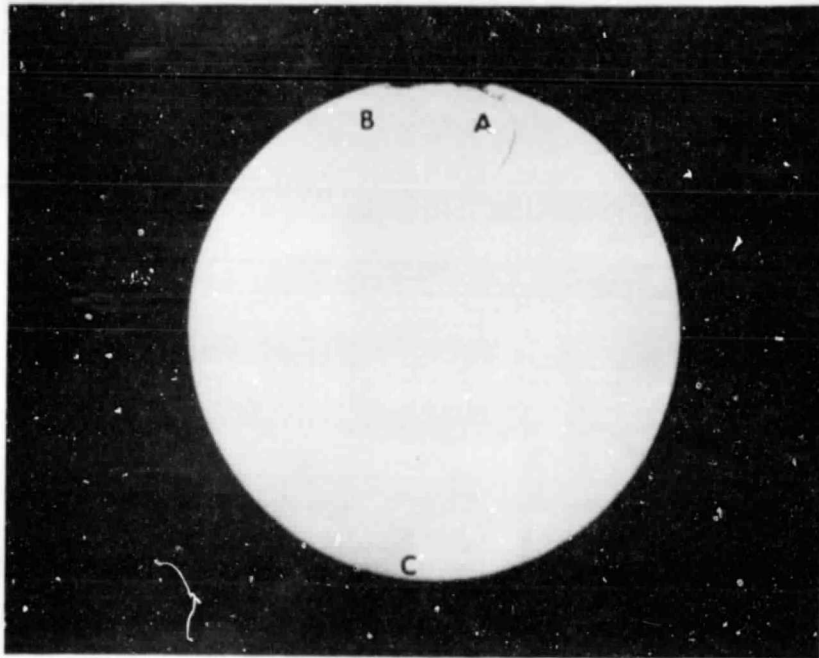


Figure 12. Cross section of spalled ball No. 4 from HPOTP 9008 bearing from Engine 2004. Cracks in areas A, B and C are shown in Figures 13, 14, and 15 respectively. Original magnification 5X.

ORIGINAL PAGE IS
OF MICROFILM

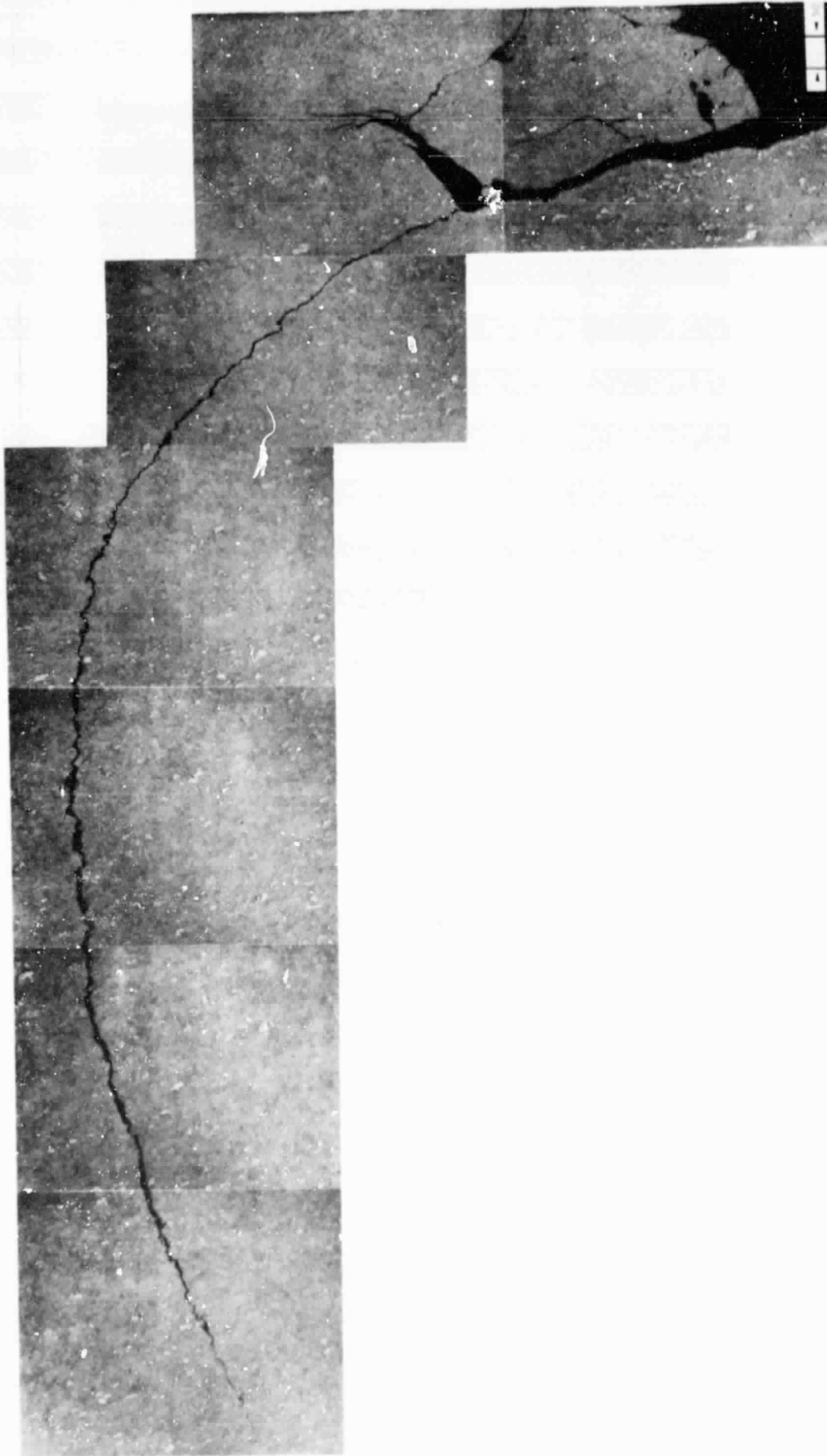


Figure 13. Deep crack in HPOTP 9008 bearing ball from Engine 2004. Crack depth approximately 2.3 mm (0.090 in.) (area A in Figure 12).

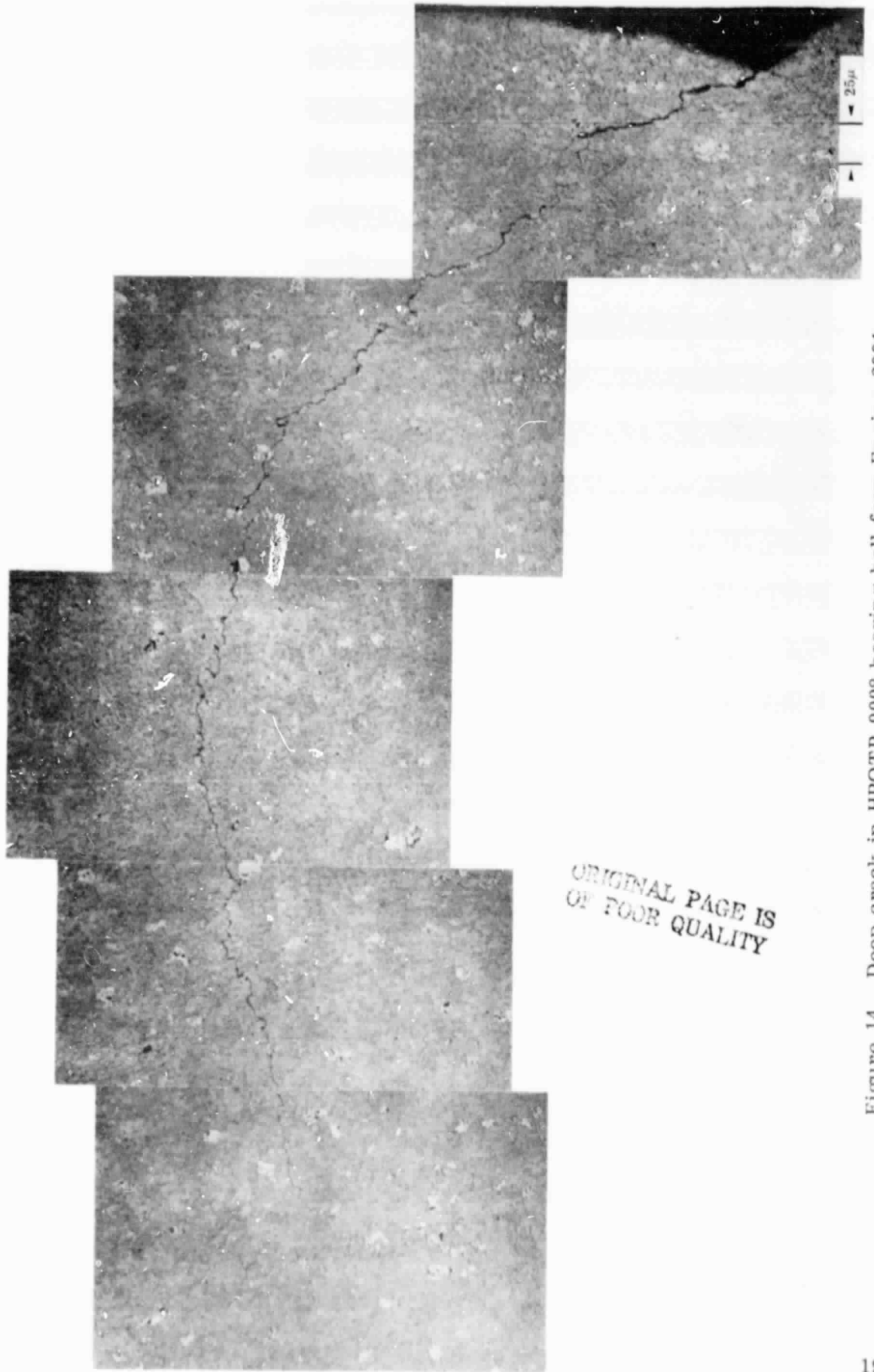
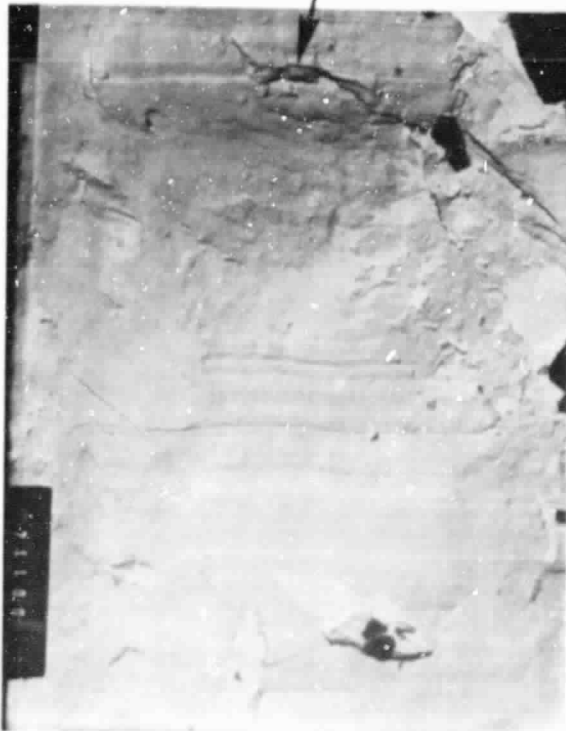


Figure 14. Deep crack in HPOTP 9008 bearing ball from Engine 2004. Crack depth approximately 0.76 mm (0.030 in.) (area B in Figure 12).

ORIGINAL PAGE IS
OF POOR QUALITY



Figure 15. Shallow crack in HPOTP 9008 bearing ball from Engine 2004.
Crack depth approximately 0.13 mm (0.005 in.) (area C in Figure 12).



ORIGINAL MAG. 6000X



ORIGINAL MAG. 18000X

Figure 16. TEM photomicrographs of fractured surface in HPOTP 9008 bearing ball from engine 2004. (Fractured surface from crack A in Figure 12).

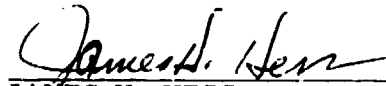
APPROVAL

FRACTURE ANALYSIS OF HPOTP BEARING BALLS

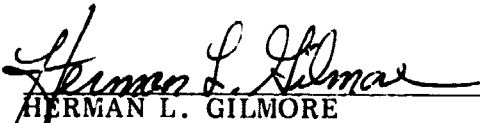
by

Biliyar N. Bhat

The information in this report has been reviewed for technical content. Review of any information concerning Department of Defense or nuclear energy activities or programs has been made by the MSFC Security Classification Officer. This report, in its entirety, has been determined to be unclassified.



JAMES H. HESS
Chief, Metallurgy Research Branch



HERMAN L. GILMORE
Chief, Metallic Materials Division



R. J. SCHWINGHAMER
Director, Materials & Processes Laboratory